

Raman Study of Isotope Effects and Phonon Eigenvectors in SiC

F. Widulle, T. Ruf, O. Buresch, A. Debernardi, and M. Cardona

Max-Planck-Institut für Festkörperforschung, Heisenbergstrasse 1, D-70569 Stuttgart, Germany
(Received 24 November 1998)

We have measured Raman spectra of several SiC polytypes (3C, 6H, 15R) made from natural silicon ($\approx^{28}\text{Si}$) and ^{30}Si . The isotope shifts of the phonon frequencies show characteristic variations with their effective wave vector in the zinc blende (3C) modification which arises from Brillouin zone backfolding. This allows us to determine the phonon eigenvectors of 3C SiC for the dispersion branches along the [111] direction. The observed magnitudes of the Si and C ion displacements, as well as their relative phase, confirm bond charge model and *ab initio* calculations. [S0031-9007(99)08863-8]

PACS numbers: 63.20.Dj, 78.30.-j

Semiconductors with controlled stable isotope composition offer exciting new possibilities for basic science and applications [1,2]. In view of the obvious mass dependence of phonon frequencies, lattice-dynamical properties have been studied intensively, mainly by Raman scattering. In addition to changes of the *average atomic mass*, *mass fluctuations* due to isotope disorder also affect phonon frequencies and linewidths. At low temperatures, isotope substitution allows one to tune the zero-point vibrational amplitudes of the nuclei which, via anharmonicity, cause changes of the lattice constant [3]. This effect and, even more important, the electron-phonon interaction lead to a renormalization of semiconductor band gaps which therefore exhibit isotope shifts. Concerning applications, the superior thermal conductivity of isotopically pure semiconductors can be exploited at places with large heat loads, e.g., in diamond monochromators for synchrotron radiation [4] and in silicon microelectronics [5].

Lately, investigations have focused on isotopic *compound* semiconductors which offer possibilities not available in elemental ones: (i) Selective isotope substitution of heavy or light constituents allows the tuning of phonon frequencies and anharmonic decay channels in different parts of reciprocal space with respect to each other due to their varying mass dependence with wave vector and phonon branch [6]. (ii) In crystals which are isotopically disordered on one sublattice, but pure on the other one, the role of the cations or anions in elastic phonon scattering can be investigated independently [1,7].

In contrast to phonon frequencies and dispersions, well known for many semiconductors, the displacement patterns, i.e., the *phonon eigenvectors*, have received much less attention. This is unfortunate since different lattice-dynamical models, although reproducing dispersion data with comparable quality, can still deviate strongly in their predictions of eigenvectors. The measurement of phonon eigenvectors thus provides possibilities for additional checks of model calculations. In addition, precise knowledge of phonon eigenvectors is required to calculate many physical properties such as inelastic neutron or light scattering intensities and selection rules.

Isotope substitution and Raman scattering have been used to determine phonon eigenvectors at the Brillouin zone center (Γ point, $k = 0$) [8,9]. This is possible in wurtzite semiconductors, such as CdS or GaN, which have coupled pairs of zone center modes with the same symmetry. In analogy to superlattices, they arise from an effective dispersion backfolding of the optic and acoustic branches along the [001] direction (Γ -A), where the unit cell is doubled compared to the zinc blende structure due to the presence of two formula units in the primitive hexagonal cell. The twice larger lattice period in real space causes a twofold reduction of the reciprocal unit cell in this direction. In a first approximation, the zinc blende dispersion can be mapped onto that of wurtzite by zone folding. The coupled pairs of Γ point phonons in the wurtzite structure can thus be considered equivalent to those of a zinc blende crystal at the L point. For the two Raman active coupled high- and low-frequency E_2 modes (the pair of B_1 modes is neither Raman nor infrared active), different isotope shifts were observed for Cd and N substitution in CdS [8] and GaN [9], respectively. From the two mode frequencies *and* their dependence on the isotope mass all three parameters of a simple lattice-dynamical model and thus the phonon eigenvectors could be determined for one high-symmetry point (L).

A limitation of first-order Raman spectroscopy is that, due to crystal-momentum conservation, only phonons at the Γ point can be investigated. *Dispersion* effects are therefore not directly accessible. While two additional modes at Γ can be studied in wurtzite, zinc blende crystals have only the usual longitudinal and transverse optic phonons whose eigenvectors are fixed by center-of-mass conservation. Here we demonstrate that *phonon eigenvectors along dispersion branches* can be measured by Raman scattering in SiC polytypes with different stable isotope composition [10]. This allows us to test theoretical predictions which, in this case, was impossible before.

SiC has long been known to form a plethora of polytypes [11,12]. These "natural superlattices" originate from different stacking sequences of hexagonally close-packed atomic planes along the [111] direction (Γ - L) of

the zinc blende (3C) modification and cover a wide range of supercell lattice constants. Because of the dispersion backfolding effects outlined above, Raman spectra of SiC polytypes may therefore exhibit several peaks related to phonons in the optic and acoustic frequency regions. An effective wave vector relative to the zinc blende Brillouin zone can be assigned to these peaks, and, to a very good approximation, this allows one to reconstruct the 3C "bulk" dispersion. In fact, all dispersion information for SiC was obtained this way by Raman scattering [11,12].

SiC crystallites were prepared by inductive heating of Si in a graphite cup under He flow to temperatures at about 2500 K. By varying the heating time and power, the preferential formation of different polytypes could be influenced. While the carbon ions, originating from the surrounding graphite, have natural isotopic composition (^{nat}C , $m_C = 12.01$ u), the mass of the silicon ions could be changed by using either natural Si (^{28}Si : 92.2%, ^{29}Si : 4.7%, ^{30}Si : 3.1%; $M_{Si} = 28.09$ u) or highly enriched ^{30}Si with an average mass of $M_{Si} = 29.85$ u according to the actual isotope composition (^{28}Si : 5.0%, ^{29}Si : 1.3%, ^{30}Si : 93.7%) determined by thermogravimetric mass spectroscopy. In micro-Raman experiments on crystals with typical dimensions at about 0.1 mm the 3C, 6H, and 15R polytypes [11,12] were identified. These measurements were performed with the samples at room temperature, using the 5145 Å Ar ion laser line.

Raman spectra for the 6H and 15R polytypes of natural SiC and ^{30}SiC are shown in Fig. 1 for the folded transverse (planar) and longitudinal (axial) optic [TO (a), LO (b)] and the corresponding acoustic [TA and LA (c)] modes. The effective wave vector coordinates q of the 3C dispersion along [111], which have been attributed to these peaks by comparison with earlier studies for natural SiC [11,12], are indicated [only the wave vector magnitudes are given, in units of π/c , where $c = \sqrt{3}a$ is the lattice constant along [111]; $\vec{q} = q(1, 1, 1)$, $0 \leq q \leq 1$]. For the $q = 0$ peaks, some extra intensity due to residual admixtures of the 3C polytype, for which the Raman signal is very strong, cannot be excluded.

Figure 2 shows the phonon dispersions of 3C SiC derived from these data (symbols). The measured isotope shifts are given by the symbols in Figs. 3(a) and 4(a). For the LO modes [Fig. 3(a)], the isotope shift decreases with increasing q , while that of the LA modes increases. The TO modes [Fig. 4(a)] have an isotope shift which is almost independent of q ; that of the TA phonons increases with increasing q . Whenever acoustic-phonon doublets were observed in the polytype spectra (see Fig. 1), their average frequency was used for the backfolding in Fig. 2 and to determine the isotope shifts in Figs. 3 and 4. Note that the backfolding of the dispersion curves could, in principle, be affected by the anisotropy of some phonons [12]. This was, however, not observed.

Investigations of the E_2 phonon eigenvectors at Γ in wurtzite CdS [8] and GaN [9] have used a simple model

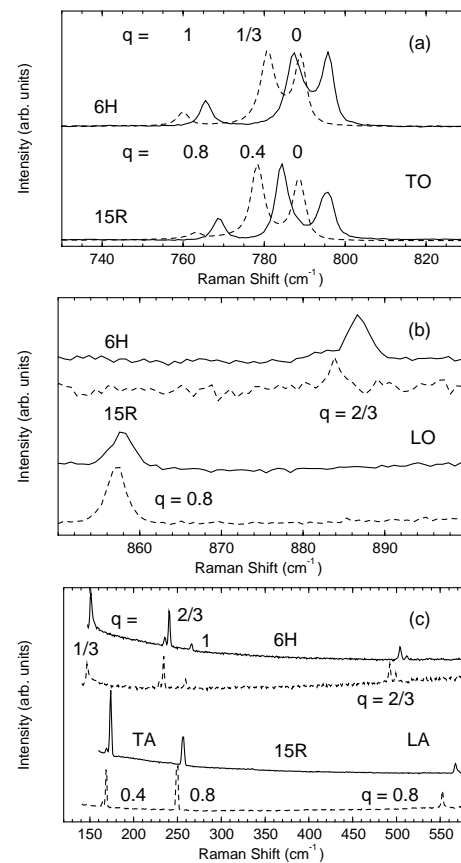


FIG. 1. Raman spectra of isotopic SiC for the 6H and 15R polytypes: (a) TO; (b) LO; (c) TA and LA phonons. The solid (dashed) line spectra refer to ^{nat}SiC (^{30}SiC). The corresponding wave vectors of the zinc blende bulk dispersion, $\vec{q} = q(1, 1, 1)$, are indicated in units of π/c .

of two coupled harmonic oscillators with mass dependences given by the heavier and lighter constituents, respectively. This approximation is justified by the fact that the two modes have significantly different frequencies, one in the acoustic and the other in the optic frequency regime. In order to describe the phonon dispersion along the [111] direction of SiC, this approach has been extended to a Born-von Kármán model with up to next-nearest neighbor interactions [10]. The lines in Fig. 2 are fits of this four-parameter model to the dispersions. They qualitatively reproduce the data. However, these fits do not reproduce isotope shifts well, and thus they are not precise enough to derive phonon eigenvectors.

We therefore separately determine the phonon eigenvectors at each q , where the maximum information, i.e., the optic and acoustic phonon frequencies and the isotope shifts for either longitudinal or transverse branches, is available. Treating the acoustic and optic phonons at arbitrary q as coupled, we solve the eigenvalue problem

$$\begin{pmatrix} -M_{Si}\omega^2 + A & C \\ C^* & -m_C\omega^2 + B \end{pmatrix} \begin{pmatrix} u_{Si} \\ u_C \end{pmatrix} = 0, \quad (1)$$

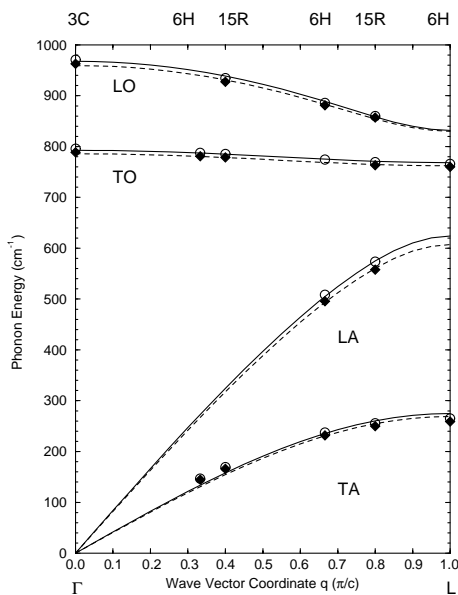


FIG. 2. Phonon dispersions of SiC determined from Raman scattering (symbols) and fits of a Born–von Kármán model [10] (lines). The Γ - L direction [$\vec{q} = q(1, 1, 1)$, $0 \leq q \leq 1$, in units of π/c] corresponds to the Brillouin zone of the zinc blende modification 3C). The open (filled) symbols [solid (dashed) lines] are data for ^{nat}SiC (^{30}SiC). The respective polytypes from which the data were obtained are indicated at the top of the figure.

with the experimental mode frequencies ω . For each q and type of phonon (longitudinal or transverse), we thus obtain a set of parameters A , B , C , and the atomic displacement vectors (u_{Si} , u_C) can be determined.

In order to compare our results with recent theoretical studies, we use the phonon eigenvectors (e_{Si} , e_C) = ($M_{Si}^{1/2} u_{Si}$, $m_C^{1/2} u_C$) and the convention

$$e_C = e(C) \exp[i\Phi(C)], \quad [e(C) \geq 0],$$

$$e_{Si} = \sqrt{1 - e(C)^2} = e(Si) \quad (2)$$

for the acoustic modes [13,14]. The eigenvectors of the optic modes can be obtained by the replacements $\Phi \rightarrow \Phi + \pi$ and $e(C) \leftrightarrow e(Si)$.

The magnitudes and phases of the eigenvectors for the longitudinal and transverse acoustic phonons determined by this procedure are given by the symbols in Figs. 3(b) and 4(b), respectively. We estimate an error of about 10% in the relative contribution of each species to the experimental eigenvectors. Note that away from the high-symmetry points Γ and L , the eigenvectors are complex numbers, i.e., $\Phi \neq 0, \pi$. For the longitudinal modes, the weight of the ion dominating the vibration at Γ (Si for the acoustic and C for the optic branch) increases with increasing q while that of the minor admixture decreases. At the same time, the isotope shift of the LO branch [see Fig. 3(a)] decreases and that of the LA increases. This highlights the close relation between isotope shifts and

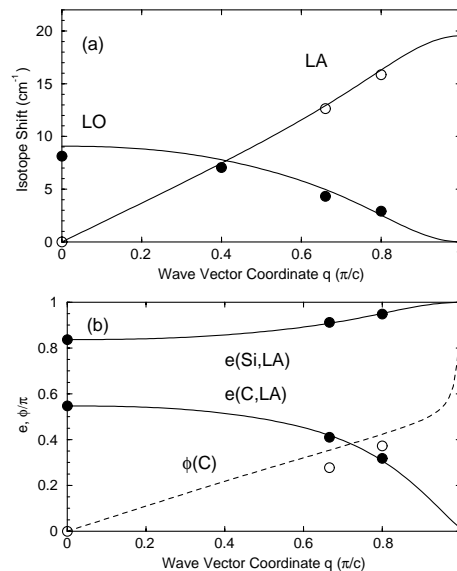


FIG. 3. Isotope shifts (a) and phonon eigenvectors (b) of the longitudinal modes along the Γ - L direction of the Brillouin zone in 3C SiC. The circles in (a) denote the measured shifts; those in (b) are data obtained from the diagonalization of Eq. (1). The lines are calculated isotope shifts (a) [Eq. (3)] and eigenvectors (b), given by a magnitude and a phase (from Refs. [13,14]). See text for details.

eigenvectors, expressed in perturbation theory as [15]

$$\frac{\partial \omega}{\partial M_i} = -\frac{\omega}{2M_i} \sum_{\alpha} |e_{i,\alpha}|^2 \quad (\alpha = x, y, z), \quad (3)$$

where i denotes the atomic species considered. For the transverse phonons [see Fig. 4(b)], only a small increase in the weight of the dominating admixture of the modes is

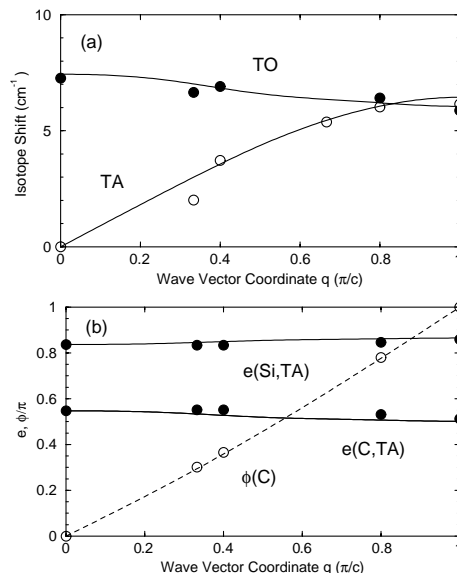


FIG. 4. Isotope shifts (a) and phonon eigenvectors (b) of the transverse modes along Γ - L in 3C SiC. See caption of Fig. 3 and the text for details.

observed as q changes from 0 to π/c (L point) and that of the minor admixture decreases only slightly. This is expected in view of the rather small decrease of the TO shift observed in Fig. 4(a) and Eq. (3).

The solid and dashed lines in Figs. 3(b) and 4(b) represent *ab initio* calculations of the lattice dynamics in 3C SiC [14,16]. The solid lines in Figs. 3(a) and 4(a) were calculated with Eq. (3) using these eigenvectors that were taken from Ref. [14]. These calculations are confirmed by our measurements. The *ab initio* data are quite close to the results of a bond charge model calculation (see Fig. 6 of Ref. [13] which are not reproduced here but also describe our findings well. At Γ , both optic modes exhibit a reduced-mass behavior with $(e_{Si}, e_C) = (0.55, -0.84)$, as required by center-of-mass conservation.

At the L point, the calculations yield an almost vanishing isotope shift for the LO phonon and an eigenvector with an almost pure carbon displacement. The large isotope shift of the LA phonon at L reflects the fact that this mode consists of almost pure Si displacements. This is similar to the behavior along [100], where the frequencies and eigenvectors at the zone edge (X point) depend *only* on the light and heavy atom mass for optic and acoustic frequencies, respectively, but at the Γ point they scale with the reduced mass. At the X point, this is required by symmetry. However, small differences may occur at L because the symmetry restriction does not hold (no reflection plane perpendicular to the [111] direction).

The calculations extrapolate the experiments to the Brillouin zone edge. Measurements could not be performed there due to the absence of polytypes with Raman active modes at $q = \pi/c$, such as $4H$ or $8H$, in our samples [11,12]. This lack of experimental information also includes the phase Φ which, for the acoustic modes, could approach either 0 or π at the L point in SiC, depending on whether the restoring force constants of this compound semiconductor are more related to the elemental parent materials of silicon or diamond, respectively [14]. Microscopically, this difference arises from the varying relative importance of bond stretching and bending contributions to the phonon frequencies [14]. The measured phase at $q = 0.8\pi/c$ [see Fig. 3(b)] is significantly larger than that determined experimentally for Si [17]. This makes it likely that $\Phi \rightarrow \pi$ at the L point for the acoustic modes in SiC as in diamond [18], where bond bending dominates, but opposite to Si ($\Phi \rightarrow 0$) [17], where bond stretching is more important. Note, however, that Φ is not defined when one of the eigenvector components at L is exactly zero. Therefore, the theoretical results at L should not be accepted as correct without experimental confirmation on appropriate polytypes even though they are suggested by the present measurements.

The small decrease of the reduced-mass shift of the TO phonon at Γ along the [111] direction [see Fig. 4(a)] indicates a significant admixture of Si and C displacements

in the eigenvectors [see Fig. 4(b)]. The measured TO eigenvector at the L point is $(e_{Si}, e_C) = (0.51, 0.86)$, in excellent agreement with the calculations. In contrast to the longitudinal modes, information at L can be obtained here since TO and TA phonons are Raman active in the $6H$ polytype available to us [11,12]. Note that the phase for the acoustic modes varies continuously between 0 at Γ and π at L [see Fig. 4(b)]. The observation that the Si and C displacements at the L point are in phase for the TO phonon reflects the dominance of bond stretching contributions to the phonon frequency in SiC, as is the case for both diamond and silicon.

From isotope shifts in the Raman spectra of SiC polytypes we have determined phonon eigenvectors (both magnitude and phase) for the zinc blende modification along the Γ - L direction. Our results confirm *ab initio* and bond charge model phonon calculations. This study could be complemented by measurements on samples with different carbon isotopes.

We thank P. Hiessl, H. Hirt, and M. Siemers for technical assistance, A. Schmeding for determining the isotope composition of the ^{30}Si , and P. Pavone for providing files with the phonon eigenvectors of Ref. [14].

-
- [1] A. Göbel *et al.*, in *Proceedings of the 24th International Conference on the Physics of Semiconductors* (World Scientific, Singapore, to be published).
 - [2] M. Cardona, *Physica* (Amsterdam) **263B-264B**, 376 (1999).
 - [3] A. Kazimirov *et al.*, *Science* **282**, 930 (1998).
 - [4] L.E. Berman *et al.*, *Synchrotron Radiation News*, **6**, No. 3, 21 (1993).
 - [5] W.S. Capinski *et al.*, *Appl. Phys. Lett.* **71**, 2109 (1997).
 - [6] A. Göbel *et al.*, *Phys. Rev. B* **56**, 210 (1997).
 - [7] A. Göbel *et al.*, *Phys. Rev. B* **59**, 2749 (1999).
 - [8] J.M. Zhang *et al.*, in *The Physics of Semiconductors*, edited by M. Scheffler and R. Zimmermann (World Scientific, Singapore, 1996), p. 201.
 - [9] J.M. Zhang *et al.*, *Phys. Rev. B* **56**, 14399 (1997).
 - [10] F. Widulle *et al.*, in *Proceedings of the 24th International Conference on the Physics of Semiconductors* (World Scientific, Singapore, to be published).
 - [11] D.W. Feldman *et al.*, *Phys. Rev.* **173**, 787 (1968).
 - [12] S. Nakashima and H. Harima, *Phys. Status Solidi* (a) **162**, 39 (1997), and references therein.
 - [13] M. Hofmann *et al.*, *Phys. Rev. B* **50**, 13401 (1994).
 - [14] K. Karch *et al.*, *Phys. Rev. B* **50**, 17054 (1994).
 - [15] J. Menéndez *et al.*, *Philos. Mag. B* **70**, 651 (1994).
 - [16] A. Debernardi and M. Cardona, *Il Nuovo Cimento* **20D**, 923 (1998).
 - [17] D. Strauch *et al.*, *Z. Phys. B* **78**, 405 (1990); J. Kulda *et al.*, *Phys. Rev. B* **50**, 13347 (1994).
 - [18] J. Kulda *et al.*, *Physica* (Amsterdam) **234B-236B**, 124 (1997).